Charge Transport in Molecular Electronic Junctions: Compression of the Molecular Tunnel Barrier in the Strong Coupling Regime

Sayed Y. Sayed[1§], Jerry A. Fereiro1[§], Haijun Yan[2], Richard L. McCreery[1,2], and Adam Johan Bergren[2*]

1. Department of Chemistry, University of Alberta, Edmonton, Alberta, Canada

2. National Institute for Nanotechnology, National Research Council Canada, Edmonton, Alberta, Canada

[§]These authors contributed equally to this work.

*corresponding author: adam.bergren@nrc.ca

Supporting information to "Charge Transport in Molecular Electronic Junctions: Compression of the Molecular Tunnel Barrier in the Strong Coupling Regime"

Introduction

This document contains additional supporting data, figures, discussions, and equations that are used to support the main text. Specifically:

1. *J-V* curves for all of the molecules tested as a function of thickness.
2. Statistical analysis carried out for the uncertainty in the beta values.
3. Determination of $E_{HOMO,onset}$ for different molecules.
4. Energy level diagram constructed from UPS data.
5. Overlay of UPS spectra of different thicknesses of NAB on carbon.
6. Example of Simmons Fitting.
7. Overlay of UPS spectra of NAB molecule on different substrates.
8. Table for the different molecules used and the number of junctions tested.
9. Sample fabrication details, including conditions used to form molecular films.
10. Measuring film thickness using AFM.

Supporting information to "Charge Transport in Molecular Electronic Junctions: Compression of the Molecular Tunnel Barrier in the Strong Coupling Regime"

1. *J-V* curves

Figure S1 shows the *J-V* curves for the different aromatic molecules (1-AQ, BTB, 2-AQ, BrP, AB, NAB) covalently bonded to carbon, as a function of thickness. The data for AB and NAB are from published results (citation 19 in the main text)

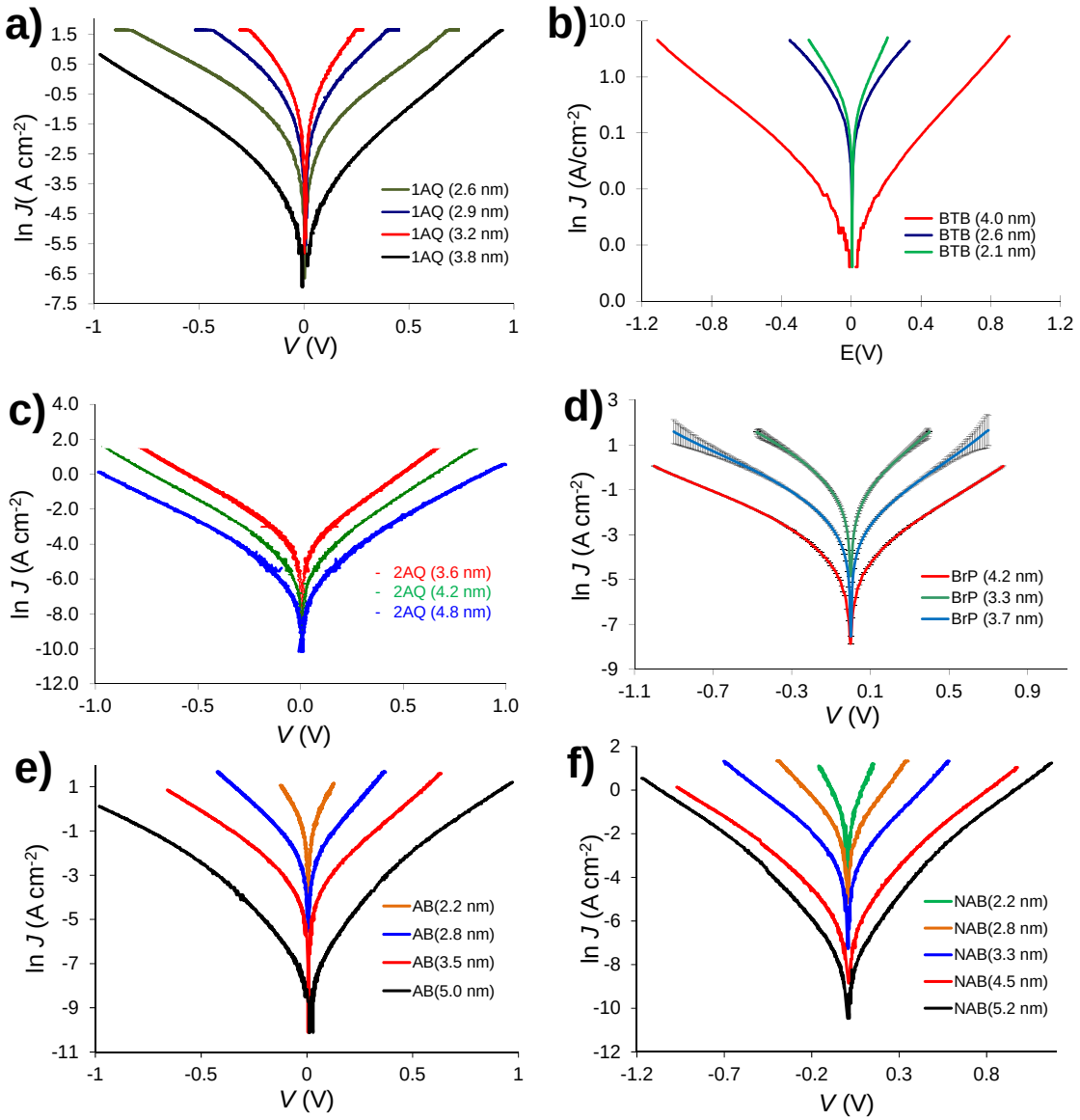

Figure S1. *J-V* curves for 1AQ (a), BTB (b), 2AQ (c), BrP (d), AB (e) and NAB (f) as a function of thickness. Error bars for J ($\pm \sigma$) are included, but are smaller than the width of the lines for all molecules except BrP. Data for AB and NAB reproduced with permission from Bergren, A. J.; McCreery, R. L.; Stoyanov, S. R.; Gusarov, S.; Kovalenko, A. *J. Phys. Chem. C* **2010**, *114*, 15806. Copyright (2010) American Chemical Society.

2. Statistical Analysis

For each molecule the number of points used to obtain the beta value (n_i) is noted and then the standard deviation for each β value ($\boldsymbol{\sigma_\beta}$) is determined, with only the layer thickness error contributing significantly to σ_β. The uncertainty in the thickness from AFM measurements is typically 0.6 nm (see below), and this value was used in all cases. Using this value for the uncertainty in thickness yields the values listed in Table 1 of the main text and Table S-1 below for the σ_β in β via the equation (from the 2nd edition of An Introduction to Error Analysis by John R. Taylor, pages 184-190):

Equation S-1

$$\sigma_\beta = 0.6\sqrt{\frac{n}{n\sum d_i^2 - (\sum d_i)^2}}$$

where n is the number of data points in the attenuation plot and d_i is the thickness of each molecular layer used to generate the attenuation plot.

In order to determine if two β values are significantly different from each other given the values of σ_β, a Student's-t analysis is carried out at the 95% confidence level. To begin, the equation to determine $\boldsymbol{\sigma}_{\text{pooled}}$ for the two data sets being compared is given below (from the 4th edition of Quantitative Chemical Analysis by Daniel C. Harris, page 67):

Equation S-2

$$\sigma_{\text{pooled}} = \sqrt{\frac{\sigma_1^2(n_1 - 1) + \sigma_2^2(n_2 - 1)}{n_1 + n_2 - 2}}$$

Where $\boldsymbol{\sigma}_i$ is the standard deviation for beta as calculated above for a given molecule and n_i is the number of data points in each attenuation plot. The values obtained for $\boldsymbol{\sigma}_{\text{pooled}}$ are given in Table S-2. The value for the student's-t value (t_{calc}) is determined using the formula given below (from the 4th edition of Quantitative Chemical Analysis by Daniel C. Harris, page 67):

Equation S-3

$$t_{\text{calc}} = \frac{\bar{x}_1 - \bar{x}_2}{\sigma_{\text{pooled}}}\sqrt{\frac{n_1 n_2}{n_1 + n_2}}$$

Where $\bar{\beta}_i$ is the average value for β for a given molecule, and the other parameters have been defined previously. The value calculated from Equation S-3 are then compared with the $t_{95\%}$ value for a given degree of freedom ($n_1 + n_2 - 2$) listed on page 63 of the 4th edition of Quantitative Chemical Analysis by Daniel C. Harris. These results are given in Table S-3, where red highlighting indicates a statistical difference in β values at the 95% confidence level. Here, a clear difference is seen between the beta values for aromatic series with that of aliphatic series. However, we do not have sufficient evidence here to claim any differences between the aromatic molecules. A possible difference is indicated

in 3 out of 36 comparisons, but these differences are not robust enough to make any claims. That is, $t_{95\%}$ = 2.447 and 2.365 for 6 and 7 degrees of freedom respectively. For one of these comparisons, the value of t_{calc} is 2.53 (6 dof), and 2.47 and 2.94 (7 dof) in the other two cases.

Table S-1. Summary of the number of points in the attenuation plot for each molecule, the average value of β, and the resulting standard deviation in β calculated using Equation S-1.

npts	molecule	β	σ_β
3	EtBen	2.1	0.7
4	NP	2.7	0.6
4	BrP	3.7	0.9
4	1AQ	3.3	0.7
3	2AQ	2.1	0.7
3	BTB	2.9	0.4
4	AB	2.5	0.3
5	NAB	2.5	0.2
3	C8	8.7	1.8

Table S-2: calculated values for σ_{pooled}.

σ_{pooled}									
	EtBen	NP	BrP	1AQ	2AQ	BTB	AB	NAB	alkanes
EtBen									
NP	0.641872								
BrP	0.825833	0.764853							
1AQ	0.7	0.65192	0.806226						
2AQ	0.7	0.641872	0.825833	0.7					
BTB	0.570088	0.52915	0.74162	0.598331	0.570088				
AB	0.5	0.474342	0.67082	0.538516	0.5	0.343511			
NAB	0.43589	0.420883	0.608276	0.482553	0.43589	0.282843	0.247848		
C8	1.36565	1.229634	1.334916	1.260952	1.36565	1.30384	1.161895	1.051982	

Table S-3. Student's t-values for comparison of β values for different molecules. Those that are greater than $t_{95\%}$ are highlighted.

t_{calc}									
	EtBen	NP	BrP	1AQ	2AQ	BTB	AB	NAB	alkanes
EtBen									
NP	1.223895								
BrP	2.536702	1.849001							
1AQ	2.244527	1.301583	0.701646						
2AQ	0	1.223895	2.536702	2.244527					
BTB	1.718676	0.494872	1.412376	0.875306	1.718676				
AB	1.047446	0.596285	2.529822	2.100903	1.047446	1.524616			
NAB	1.256562	0.708373	2.940858	2.471377	1.256562	1.936492	0		
C8	5.919025	6.388766	4.904082	5.607081	5.919025	5.448151	6.986609	8.070193	

Supporting information to "Charge Transport in Molecular Electronic Junctions: Compression of the Molecular Tunnel Barrier in the Strong Coupling Regime"

3. Determination of $E_{HOMO,onset}$

UPS spectra used for the determination of $E_{HOMO,onset}$ values for different molecules given in Table 2 in the main text, as described recently by Kim et al. (1).

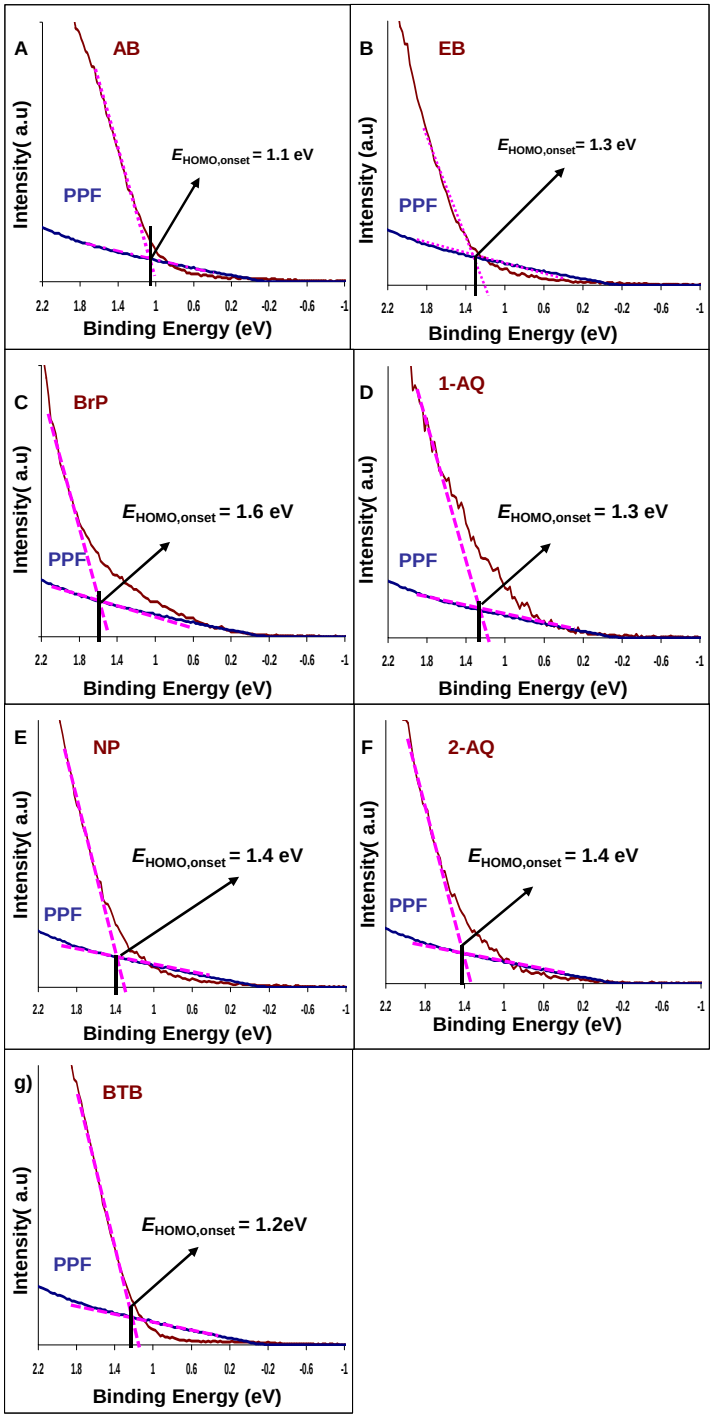

Figure S2. UPS spectra used for the determination of $E_{HOMO,onset}$ values for different molecules: AB, EB, BrP, 1-AQ, 2-AQ, NP and BTB.

4. Energy Level Diagram

Using the UPS HBEC, the following diagram is constructed to represent the energy level shifts upon bonding a molecule to PPF:

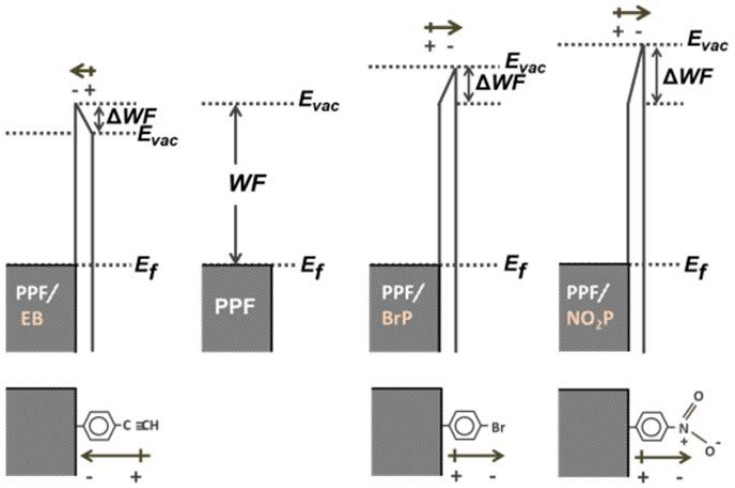

Figure S3. Energy level diagram showing the vacuum level shift induced by the molecular dipole for the molecules shown in Figure 5 of the main text.

5. UPS Spectra as a Function of Thickness

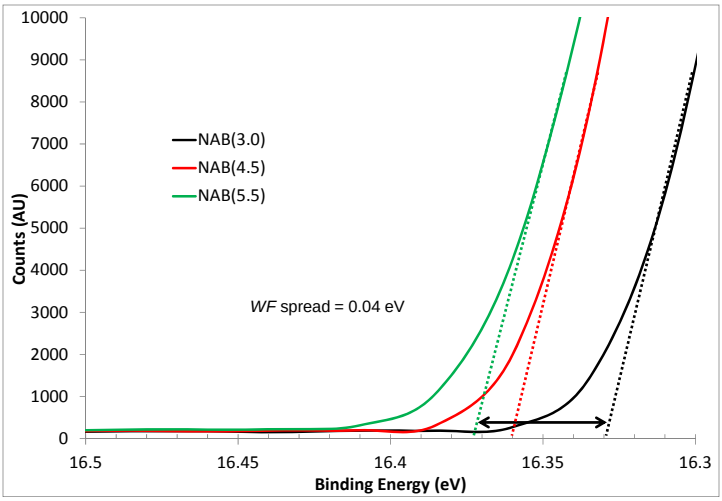

Figure S4. UPS spectra in the HBEC region for NAB as a function of thickness, showing a variation of less than 0.05 eV for the range of 3.0 to 5.5 nm.

6. Example of Simmons Fitting

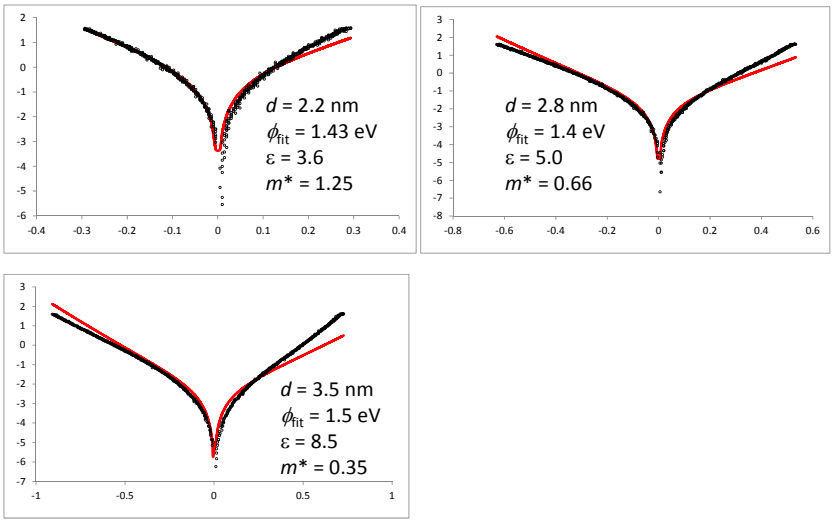

Figure S5. *J-V* curves for different thicknesses of EB fit to the Simmons model. The black dots are the experimental data, while the red lines are the results of the full Simmons model, implemented as described previously (2), where the parameters obtained are indicted. Fits for all of the molecules in the main text are available upon request.

7. Overlay of UPS Spectra for NAB on Different Substrates

Overlay of UPS spectra for NAB molecule by modifying samples of carbon, gold and platinum.

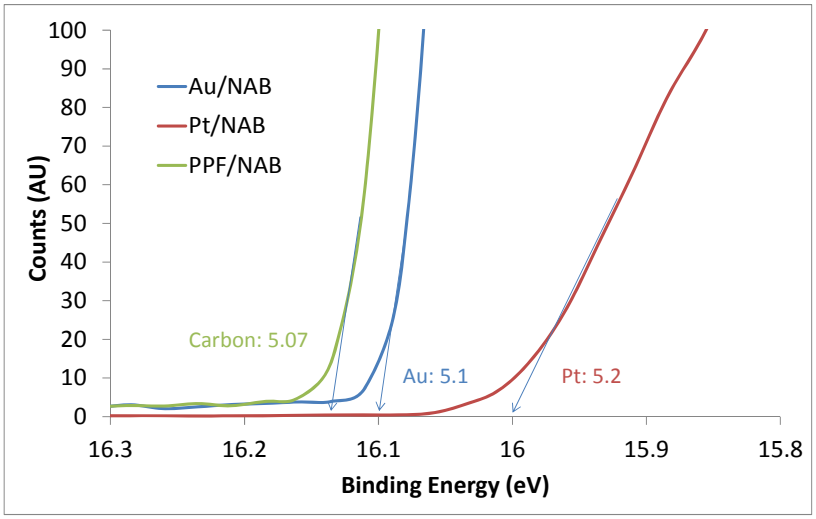

Figure S6. UPS spectra in the HBEC region for NAB on three different metals. Numbers in figure are the measured WF for each sample obtained by 21.21 eV minus the x-axis intercept (i.e., the HBEC).

8. Number of Junctions

Table S4. Summary of the number of junctions made for each molecule. We note that AB (2), NAB (2), and the alkane (3) data were previously published.

Molecule	No: of Junctions tested
EB	24
NP	64
BrP	64
BrP	32
1AQ	96
2AQ	72
BTB	24
AB	32
NAB	40
Alkanes	24

9. Sample Fabrication and Conditions for Film Growth

Conductive carbon films were made on thermally oxidized silicon chips (200 nm oxide layer) by the pyrolysis of four parallel photolithographically patterned photoresist lines (0.5 mm wide). After pyrolysis, the conductive pyrolyzed photoresist films (PPF) were modified with nanoscopic molecular layers by the electrochemical reduction of diazonium ions. The PPF was the working electrode in a 1 mM solution of the diazonium precursor (with N_2^+ on the lowest ring position shown in Figure 2 of the main text) with 0.1 M tetrabutylammonium tetrafluoroborate as the supporting electrolyte in acetonitrile. Cyclic voltammetric sweeps were initiated from a potential at which no reduction occurs (generally +0.4 V versus Ag/Ag^+) to a negative potential at which electrolysis proceeds. The cathodic switching potential depends on the molecule used and the desired thickness (see SI section 10). For BTB, an in-situ technique was used to generate the diazonium ion (4, 5). After rinsing with acetonitrile and drying in a stream of nitrogen, the samples were transferred to the vacuum chamber of an electron beam evaporation system. Top contact (30 nm Cu and 15 nm Au) deposition was carried out through shadow masks with 0.25 mm wide rectangular openings oriented perpendicular to the PPF lines to result in a cross-bar junction of ~0.0013 cm^2 area. Typically, each chip contains 4-8 measureable junctions, and the conductance of each molecular layer is reported as the average of the *J-V* measurements across each chip.

The general conditions used for film growth are given below. We note that due to the large number of experimental variables, the thickness must always be verified using AFM (see below). These conditions are indicative of what we have used to produce the molecular layers in this work and can serve as a guide for others.

In all cases except BTB, the carbon surface (PPF) is used as the working electrode in a three-electrode electrochemical cell in a dilute solution (1.0 mM) of diazonium precursor (2.0 mM for both 1-, and 2-AQ) in acetonitrile (with 0.1 M tetrabutylammonium tetrafluoroborate as supporting electrolyte). Electrografting was performed by sweeping the electrode potential at a rate of 0.1 or 0.2 V s^{-1} from a potential where no reduction occurs (+0.4 V vs Ag/Ag^+) to a negative voltage of -0.6 V for AB, NAB, 1AQ, and 2AQ and of -1.1 V and -1.2 V for NP and BrP, respectively. In the case of EB, potential sweep was done from 0.3 to -0.8 V. The thickness of the molecular multilayer (1-5nm) was varied by varying reduction switching potential from -0.4 to -0.6 V (for AB, NAB, 1AQ, and 2AQ), -1.0 to -1.1 V (for NP), and -1.0 to -1.2 V (for BrP) and the number of cycles from 1 to 10 for all cases except EB, for which the number of cycles was changed from 2 to 6.

In situ diazonium formation of BTB: An acetonitrile (ACN) solution (20mL) containing 4-amino-1-bisthienylbenzene (5mM, ~2.6mg) and tetrabutylammonium tetrafluoroborate ($TBABF_4$, 0.1M, ~0.66g) as supporting electrolyte was prepared and degassed with high purity Ar for ~30 minutes. Tert-butylnitrite (18μL) was then added to the above solution and was stirred for 15 min before electrografting was started. The diazonium salt concentration may vary with time. After surface modification, samples were thoroughly rinsed with copious ACN and dried with Ar.

Samples for ultraviolet photoelectron spectroscopy (UPS) were prepared using non-patterned PPF chips, with molecular layer depositions carried out in the same manner as for the patterned chips used for junction fabrication. UPS spectra were acquired using a Kratos Ultra spectrometer with a He I source (21.21 eV) and a pass energy of 5 eV at normal take off angle and represent the average of 12 scans (6). In addition to measuring many different molecular structures on PPF, a single structure (NAB, see Figure 2 below) was also measured after depositing onto several different substrate materials in the same manner.

10. Measurement of Molecular Layer Thickness

Film thicknesses were measured using the actual junction samples. First, using contact mode, a ~1 x 1 μm trench was made in the molecular layer using a set point which removed the molecules but did not damage the underlying carbon (this was checked for several samples by using the same set point on unmodified PPF). A 5 x 5 μm tapping mode image was then obtained in the area surrounding and including the trench. Finally, the image was analyzed to determine the difference in height between the bottom of the trench and the upper surface of the molecular layer. A histogram generated from the height data was fit by two separate Gaussian functions (for the two different height distributions), with the height determined as the difference between the centres of the two functions and the uncertainty given as the quadrature addition of the two best-fit σ values. It is important to note that the measurement of thickness is by far the largest source of uncertainty in our data. Typically, the standard deviation of the thickness determined from AFM was between 0.5 and 0.6 nm (i.e., for a 4.0 nm thickness, this is a 15% relative error). In order to draw statistically valid conclusions, we have accounted for this experimental error in our data analysis.

Figure S-7 shows a 5 x 5 μm tapping mode image including the trench and the surrounding area. Figure S-8 shows the histogram generated from the height data fit by two different Gaussian functions. Thicknesses stated in main text are the difference of the centers of the Gaussian distribution, with the uncertainty in thickness stated as the quadrature addition of the two best-fit σ values. The overall average for thickness measurements carried out in this way is ~0.55 nm (this is the average value obtained for 9 samples for illustrative purposes).

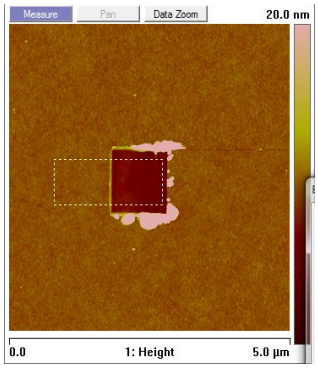

Figure S7.AFM image of a trench made in a molecular layer of nitro phenyl on carbon (PPF).

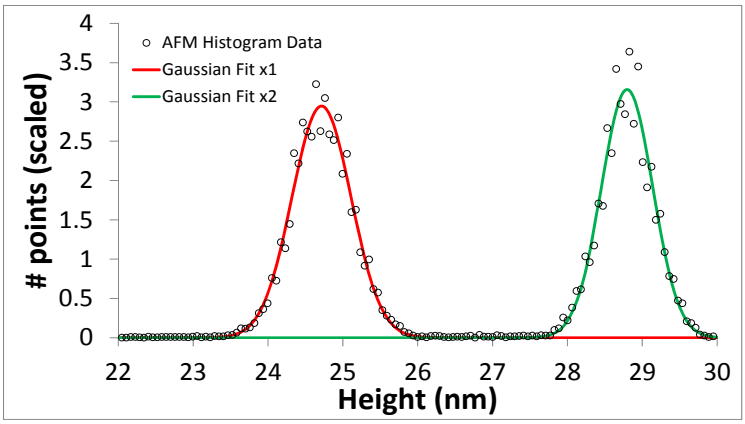

Figure S8.Fitting of the date generated as a histogram from the AFM data shown in Figure S7.

References

1. Kim B, Choi SH, X.-Y.Zhu, & Frisbie CD (2011) Molecular Tunnel Junctions Based on π-Conjugated Oligoacene Thiols and Dithiols between Ag, Au, and Pt Contacts: Effect of Surface Linking Group and Metal Work Function. *J. Am. Chem. Soc.* 133(49):19864-19877.
2. Bergren AJ, McCreery RL, Stoyanov SR, Gusarov S, & Kovalenko A (2010) Electronic Characteristics and Charge Transport Mechanisms for Large Area Aromatic Molecular Junctions. *J. Phys. Chem. C* 114(37):15806-15815.
3. Bonifas AP & McCreery RL (2010) "Soft" Au, Pt and Cu contacts for molecular junctions through surface-diffusion-mediated deposition. *Nat. Nanotechnol.* 5(8):612-617.
4. Martin P, Rocca MLD, Anthore A, Lafarge P, & Lacroix J-C (2012) Organic Electrodes Based on Grafted Oligothiophene Units in Ultrathin, Large-Area Molecular Junctions. *J. Am. Chem. Soc.* 134:154-157.
5. Fave C, *et al.* (2007) Tunable Electrochemical Switches Based on Ultrathin Organic Films. *J. Am. Chem. Soc.* 129:1890-1891.
6. Yan H, Bergren AJ, & McCreery RL (2011) All Carbon Molecular Tunnel Junctions. *J. Am. Chem. Soc.* 133(47):19168-19177.